

Copy

RM A9C16

~~CONFIDENTIAL~~

NACA RM A9C16

A 9C16

NACA

0142949

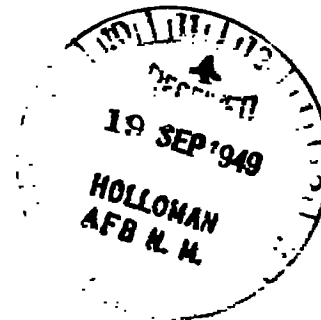
TECH LIBRARY KAFB, NM

# RESEARCH MEMORANDUM

A COMPARISON OF THEORETICAL AND EXPERIMENTAL  
LOADING ON A  $63^\circ$  SWEPT-BACK WING  
AT SUPERSONIC SPEEDS

By Victor I. Stevens and John W. Boyd

Ames Aeronautical Laboratory  
Moffett Field, Calif.



NATIONAL ADVISORY COMMITTEE  
FOR AERONAUTICS

WASHINGTON  
September 14, 1949

319.981/13



## NATIONAL ADVISORY COMMITTEE FOR AERONAUTICS

RESEARCH MEMORANDUM

## A COMPARISON OF THEORETICAL AND EXPERIMENTAL

LOADING ON A  $63^\circ$  SWEEP-BACK WING

## AT SUPERSONIC SPEEDS

By Victor I. Stevens and John W. Boyd

## SUMMARY

The pressure distribution over a highly swept wing has been investigated at supersonic speeds to provide data for a comparison of measured and predicted loadings. The wing for this investigation had  $63^\circ$  sweepback of the leading edge, an aspect ratio of 3.5, and a taper ratio of 0.25. The experimental data were obtained for Mach numbers from 1.15 to 1.70 at a Reynolds number of approximately 4.5 million and angles of attack to  $10^\circ$ .

The measured loading is compared with that predicted by use of supersonic lifting-surface theory. Over the region of the wing not affected by the wing trailing edge or tip, the results are essentially in accord with those of NACA RM A8F22; that is, theory and experiment are generally in good agreement. Over the remainder of the wing, the agreement between theory and experiment is not good but is much better than that found in NACA RM A8F22. This improvement in the agreement is attributed to differences in airfoil section.

## INTRODUCTION

The aerodynamic theory developed to date for predicting the loading on wings in supersonic air streams has necessarily involved certain simplifying assumptions. The two principal simplifications are (1) linearization of the equations of motion, and (2) omission of viscosity effects. It follows that a number of checks between loadings obtained by theory and experiment are needed to determine to what extent the foregoing assumptions limit the applicability of the theoretical methods and, if possible, to develop procedures for extending the range of usefulness of the theory.

One such check is afforded by reference 1 which compares the loadings predicted by the method of reference 2 and those measured for an untapered  $63^\circ$  swept-back wing at a Mach number of 1.53. Good agreement between theory and experiment was indicated except near the tip and the trailing edge. The discrepancy at the tip was apparently due, at least in part, to the fact that the linear theory does not properly account for the flow around a wing tip. The lack of agreement near the trailing edge was attributed to boundary-layer separation.

To investigate further the correspondence between theory and experiment, the load distribution on a tapered  $63^\circ$  swept-back wing has been measured in the Ames 6- by 6-foot supersonic wind tunnel at approximately 4.5 million Reynolds number and at Mach numbers from 1.15 to 1.7. In order to facilitate early release of the data, the discussion is restricted to a few comments on the relationship between the loading measured and that predicted by the methods of references 2 and 3.

#### SYMBOLS

$\frac{\Delta p}{q}$  loading coefficient  $\left( \frac{p_l - p_u}{q} \right)$

$\frac{\Delta p}{q\alpha}$  change in loading coefficient per unit angle

of attack  $\left[ \frac{\left( \frac{\Delta p}{q} \right)_\alpha - \left( \frac{\Delta p}{q} \right)_{\alpha_{\min}}}{\alpha - \alpha_{\min}} \right]$ , per degree

$p$  local static pressure, pounds per square foot

$q$  free-stream dynamic pressure  $\left( \frac{1}{2} \rho V^2 \right)$ , pounds per square foot

$\rho$  mass density of air stream, slugs per cubic foot

$V$  velocity of air stream, feet per second

$M$  free-stream Mach number

$R$  Reynolds number based upon M.A.C. length of 11.2 inches

$\alpha$  angle of attack of the wing at the plane of symmetry, degrees

~~CONFIDENTIAL~~

- $\Delta\alpha$  increment in angle of attack of the wing at the plane of symmetry (referred to  $\alpha_{min}$ ), degrees
- $\alpha_{min}$  minimum angle of attack investigated for a given Mach number (measured at the plane of symmetry), degrees
- $\frac{x}{c}$  chordwise station, fraction of local chord measured parallel to plane of symmetry
- $\frac{y}{b/2}$  spanwise station, fraction of wing semispan measured perpendicular to plane of symmetry
- $\frac{h_{max}}{c}$  maximum wing camber as fraction of local chord
- $\bar{c}$  mean aerodynamic chord measured parallel to plane of symmetry
- $$\left( \frac{\int_{-b/2}^{b/2} c^2 dy}{\int_{-b/2}^{b/2} c dy} \right), \text{ inches}$$
- $c$  wing local chord, inches

#### Subscripts

- $l$  conditions on lower surface of wing
- $u$  conditions on upper surface of wing
- $\alpha$  conditions at the angle of attack  $\alpha$
- $\alpha_{min}$  conditions at the angle of attack  $\alpha_{min}$

#### APPARATUS

##### Wind Tunnel

The experimental investigation was conducted in the Ames 6- by 6-foot supersonic wind tunnel. This is a closed-return-type tunnel powered by two 25,000-horsepower motors coupled to an eight-stage axial-flow compressor which drives the air around the wind-tunnel circuit.

~~CONFIDENTIAL~~

Mach number, Reynolds number, and humidity are readily adjusted while the tunnel is operating. The Mach number of the air stream in the test section can be continuously varied from 1.1 to 1.8 through the use of an asymmetric sliding-block nozzle similar to that described in reference 4. The test Reynolds number is varied by changing the total pressure of the tunnel between the limits of 2 and 17 pounds per square inch absolute. The humidity of the air in the tunnel can be lowered to less than 0.0002 pound of water per pound of air by evacuating the tunnel and refilling it with dry air.

The models are mounted in the test section on the end of a cantilever sting as shown in figure 1.<sup>1</sup> The sting angle of attack can be adjusted to any angle between  $\pm 5^\circ$  while the tunnel is operating. Through use of interchangeable bent stings, various ranges of angle of attack (e.g.,  $-5^\circ$  to  $5^\circ$ ,  $0^\circ$  to  $10^\circ$ , etc.) and angles of sideslip can be obtained. For the present test, a  $5^\circ$  bent sting was employed to give an angle-of-attack range of approximately  $0^\circ$  to  $10^\circ$  at  $0^\circ$  of sideslip.

#### Model

A sketch of the model giving all the pertinent dimensions is shown in figure 2. The wing and fuselage selected for the investigation were designed for efficient flight at supersonic speeds (references 5 and 6). The fineness ratio of the body was 12.5. However, for this investigation the rear portion of the body, shown dotted in figure 2, was eliminated to allow the model to be mounted on the sting support. The wing leading edge was swept back  $63^\circ$  and the wing had an aspect ratio of 3.5 and a taper ratio of 0.25. In planes parallel to the plane of symmetry the wing consisted of NACA 64-series sections, 5 percent thick, cambered as shown in figure 3. The airfoil sections were cambered for a constant chordwise load and the wing was constructed with  $3.5^\circ$  of twist for nearly uniform surface loading at the design lift coefficient of 0.25 and the design Mach number of 1.50. The calculated mean camber line parallel to the plane of symmetry necessary to obtain a uniform chordwise load distribution was approximated in the model design by an  $a = 1.0$  mean camber line which had the same maximum camber ordinate as was determined by theory. The spanwise variation of the maximum camber is shown in figure 3 as a fraction of the wing local chord.

From considerations of Reynolds number and wind-tunnel-wall

---

<sup>1</sup>The model was inverted for this investigation.

---

interference a wing span of 35 inches was selected. A greater span would have been desirable to realize higher test Reynolds numbers but would have resulted in interference over the wing by reflection from the tunnel wall of the shock wave originating from the apex of the airfoil at the lower test Mach numbers. For the model size selected, the bow wave from the fuselage will reflect from the tunnel walls and pass across the wing at  $M \leq 1.3$ . However, its effect is believed insignificant. (See Precision, p. 6.)

To measure the loading the right wing panel was fitted with 95 pressure orifices 0.013 inch in diameter. These orifices were located in planes parallel to the plane of symmetry at five spanwise stations. (See fig. 2.)

## METHODS

### Theory

The theoretical loading for the rigid wing was calculated by the method of reference 2. In applying this method it was assumed that the basic wing lift (i.e., the lift existing over an infinite triangle having the same sweepback as the given wing) carried across the fuselage so that the flow field was conical with respect to the wing apex. However, the Mach line bounding the area affected by the trailing edge, which in reference 2 originated at the trailing edge of the wing root, was in this case assumed to originate at the juncture of the wing trailing edge and the fuselage.<sup>2</sup> The regions of the wing affected by these assumptions are shown in figure 4 for the representative Mach numbers.

In the present investigation, measurements of the deflection of the wing root and tip indicated significant distortion (twist) under load. An estimate of the effect of the deflection on the load distribution over that part of the wing unaffected by the wing trailing edge and tip has been made by using the method of reference 3 and the measured twist.

The effect of the fuselage on the wing loading per unit angle of attack was found to be negligible when investigated by the method of reference 7. Consequently, no corrections have been made for the effect of the fuselage on the theoretical load distribution.

---

<sup>2</sup>This assumes that at the juncture of the fuselage and the wing trailing edge the fuselage is, in effect, a reflection plane.

---

### Experiment

Tests.— The ranges of test variables included in this investigation were as follows:

<u>Mach number</u>	<u>Reynolds number</u>	<u>Angle of attack (nominal)</u>
1.15	$4.6 \times 10^6$	0° to 2°
1.30	$4.6 \times 10^6$	0° to 8°
1.40	$4.6 \times 10^6$	0° to 10°
1.50	$4.3 \times 10^6$	0° to 10°
1.60	$4.1 \times 10^6$	0° to 10°
1.70	$4.0 \times 10^6$	0° to 4°

In a given test the Mach number and Reynolds number were held constant while the angle of attack was varied. The pressures were indicated on multiple-tube manometers and recorded photographically. The data were directly reduced to chordwise plots of pressure coefficient through use of a pressure plotting machine.

The experimental values of  $\Delta p/q_\alpha$  were obtained by subtracting the loading coefficient for the lowest angle of attack investigated from that for a given angle of attack and dividing by the corresponding change in angle of attack. That is,

$$\frac{\Delta p}{q_\alpha} = \frac{\left(\frac{\Delta p}{q}\right)_\alpha - \left(\frac{\Delta p}{q}\right)_{\alpha_{\min}}}{\alpha - \alpha_{\min}}$$

where all angles of attack are measured at the plane of symmetry.

Precision.— Surveys of the tunnel air stream have shown the flow to be two-dimensional, that is, there are no variations of characteristics in the lateral direction. In vertical planes, however, significant variations of the static pressure, stream inclination, and curvature were measured for some Mach numbers. To determine the effects of these stream variations on the model characteristics, both the pressure distribution and the force characteristics as obtained with the model horizontal and vertical are compared in reference 8. Although changes in angle of zero lift and trim were noted, the variation of the loading, the lift and the pitching moment with angle of attack appeared to be little affected by position of the model. It is evident, therefore, that the stream conditions do not appreciably

~~CONFIDENTIAL~~

affect  $\Delta p/q\alpha$ . Since, in the present test it was more convenient to pitch the model when mounted with the wing in the horizontal plane, this position was used throughout the investigation.

Tunnel-wall interference at the low Mach numbers is another factor which may affect the precision. Of primary concern is the fact that the bow wave originating from the fuselage nose reflects from the tunnel wall and intersects the wing tip for  $M \leq 1.3$ . It might be expected that the pressures on the wing would be directly affected by the pressure rise across this reflected wave. The effect on the parameter  $\Delta p/q\alpha$  is, however, subject for argument since it involves, among other things, the reflection of the wave from the wing surface at finite angles of attack and the interaction of the wave and the wing boundary layer. Because of these factors, the magnitude of the tunnel-wall interference with respect to  $\Delta p/q\alpha$  cannot be calculated with any degree of certainty at the present time. In the present investigation, the authors believe the interference was relatively insignificant since examination of the chord-wise distribution of wing pressures revealed no irregularities in the region where the reflected wave intersected the wing.

The precision, then, in measuring  $\Delta p/q\alpha$  is affected primarily by the purely mechanical errors in measuring and reducing the data to final form. Since the experimental techniques employed in this investigation parallel those used in reference 1, it is believed that the purely mechanical errors should be approximately of the same magnitude, that is, the errors in measuring  $\Delta p/q$  should be within  $\pm 1$  percent and errors in measuring the angle of attack should be within  $\pm 0.1^\circ$ .

## RESULTS AND DISCUSSION

Experimental values of the loading per unit angle of attack are compared with theory in figures 5 to 10, inclusive, for each of the Mach numbers investigated. The predicted loading for both the rigid and elastic wings is shown in these figures.

Examination of the data in figures 5 to 10 reveals, as might be expected, that the agreement between predicted<sup>s</sup> and measured loading

---

<sup>s</sup> In this discussion the predicted loading refers to the predicted loading for the elastic wing. Although the effect of the elasticity on the wing near the tip and trailing edge is not shown, it has been assumed for the purpose of discussion that the percent reduction of the load due to elasticity would be the same as that over the forward portion of the wing.

---

is dependent upon the position on the wing surface, the angle of attack, and the Mach number. At a Mach number of 1.3 (fig. 6) and a low angle of attack ( $\Delta\alpha = 1.64^\circ$ ), the agreement is excellent at the inboard station. As the point of comparison is moved outboard and restricted to the region ahead of the trailing-edge Mach line, the measured values of  $\Delta p/q_\infty$  tend to increase slightly relative to the theoretical values. Over this same region, increases in angle of attack also tend to increase the experimental values. These same trends can be observed in the data for the other Mach numbers investigated. As the Mach number is increased, however, the measured values of  $\Delta p/q_\infty$  are reduced relative to predicted values so that, in general, theory and experiment are in better agreement at the higher Mach numbers.

According to the inviscid theory, the effects of the wing trailing edge cannot be felt ahead of the trailing-edge Mach line, and, therefore, the final pressure recovery cannot begin ahead of this line. It will be noted, however, that at the 35- and 57-percent-semispan stations for most Mach numbers and angles of attack the measured values of  $\Delta p/q_\infty$  indicate that the final pressure recovery begins ahead of the trailing-edge Mach line and is less rapid than predicted. This effect was noted in reference 1 and is apparently due to the fact that pressure signals from the trailing edge are transmitted forward ahead of the trailing-edge Mach line through the subsonic boundary layer.

It is important to note that the results of the present tests show much better agreement with theory in the region influenced by the subsonic trailing edge than the results of reference 1. It is evident that the failure of the theory to predict the angle-of-attack loading behind the trailing-edge Mach line for the model of reference 1 is due primarily to viscosity effects resulting from the excessively large trailing-edge angle of the biconvex section used. The present tests indicate that viscosity effects are still evident for the region of the airfoil influenced by the subsonic trailing edge, but inviscid theory predicts the loading with reasonable accuracy for most purposes.

For the present tests, the agreement between theory and experiment seems to be better near the tip than for reference 1 which again is probably due to the fact that the measured loadings for the model of reference 1 are influenced to a greater extent by viscosity effects.

#### CONCLUDING REMARKS

The results of this investigation show that over the portions of the wing not affected by the wing trailing edge and tip the agreement

between theory and experiment is generally good, the best agreement existing near zero lift. These results are essentially the same as those reported in NACA RM A8F22.

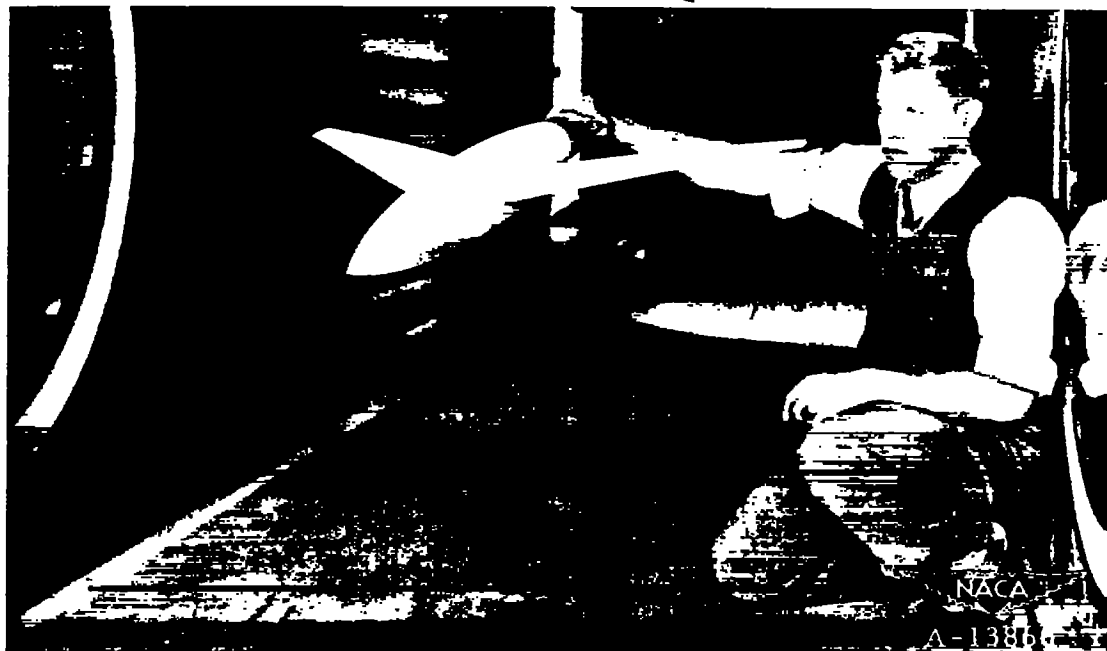
Over the regions influenced by the wing tip and trailing edge, the effects of viscosity apparently are responsible for the poorer agreement between theory and experiment. It should be noted, however, that the results of this investigation show much better agreement between theory and experiment over this region than the results of NACA RM A8F22 which indicates that airfoil section may significantly influence this agreement.

Ames Aeronautical Laboratory,  
National Advisory Committee for Aeronautics,  
Moffett Field, Calif.

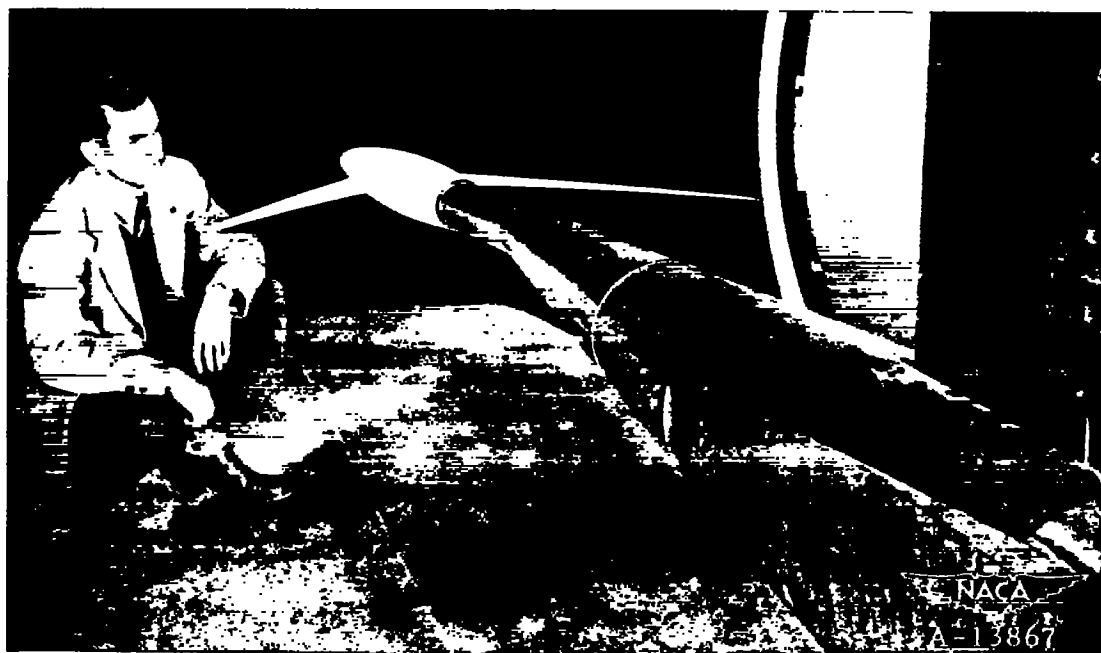
#### REFERENCES

1. Boyd, John W., Katzen, Elliot D., and Frick, Charles W.: Investigation at Supersonic Speed ( $M = 1.53$ ) of the Pressure Distribution over a  $63^\circ$  Swept Airfoil of Biconvex Section at Angles of Attack. NACA RM A8F22, 1948.
2. Cohen, Doris: The Theoretical Lift of Flat Swept-Back Wings at Supersonic Speeds. NACA TN 1555, 1948.
3. Frick, Charles W., and Chubb, Robert S.: The Longitudinal Stability of Elastic Swept Wings at Supersonic Speed. NACA TN 1811, 1949.
4. Allen, H. Julian: The Asymmetric Adjustable Supersonic Nozzle for Wind-Tunnel Application. NACA RM A8E17, 1948.
5. Madden, Robert T.: Aerodynamic Study of a Wing-Fuselage Combination Employing a Wing Swept Back  $63^\circ$ .— Characteristics at a Mach Number of 1.53 Including Effect of Small Variations of Sweep. NACA RM A8J04, 1949.
6. Jones, Robert T.: Estimated Lift-Drag Ratios at Supersonic Speed. NACA TN 1350, 1947.

7. Spreiter, John R.: Aerodynamic Properties of Slender Wing-Body Combinations at Subsonic, Transonic, and Supersonic Speeds. NACA TN 1662, 1948.
8. Frick, C. W., and Olson, R. N.: Flow Studies in the Asymmetric Adjustable Nozzle of the Ames 6- by 6-Foot Supersonic Wind Tunnel. NACA RM A9E24, 1949.

~~CONFIDENTIAL~~

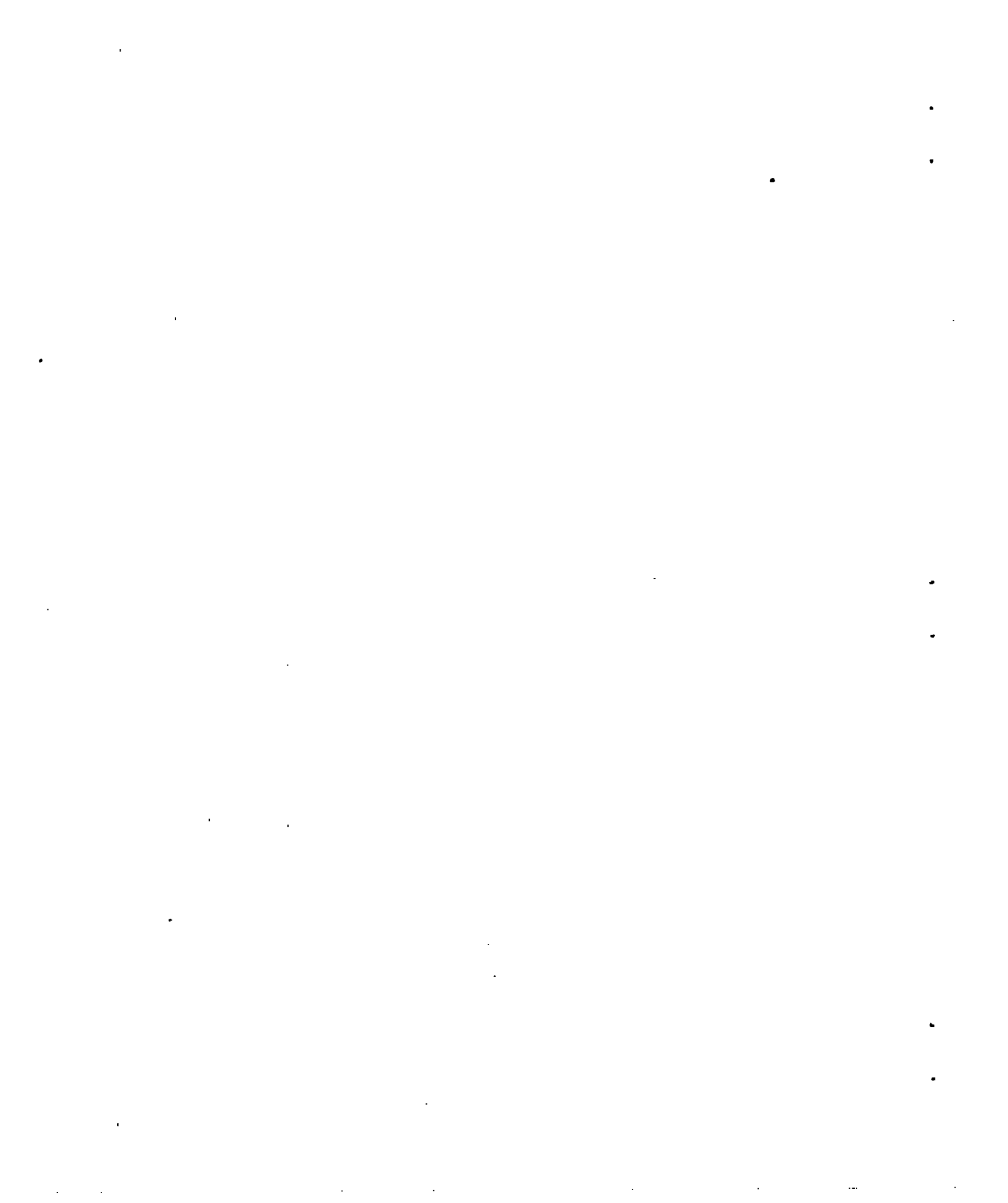
(a) Front view.



(b) Rear view.

Figure 1.- Model mounted in the Ames 6- by 6-foot supersonic wind-tunnel test section.

~~CONFIDENTIAL~~



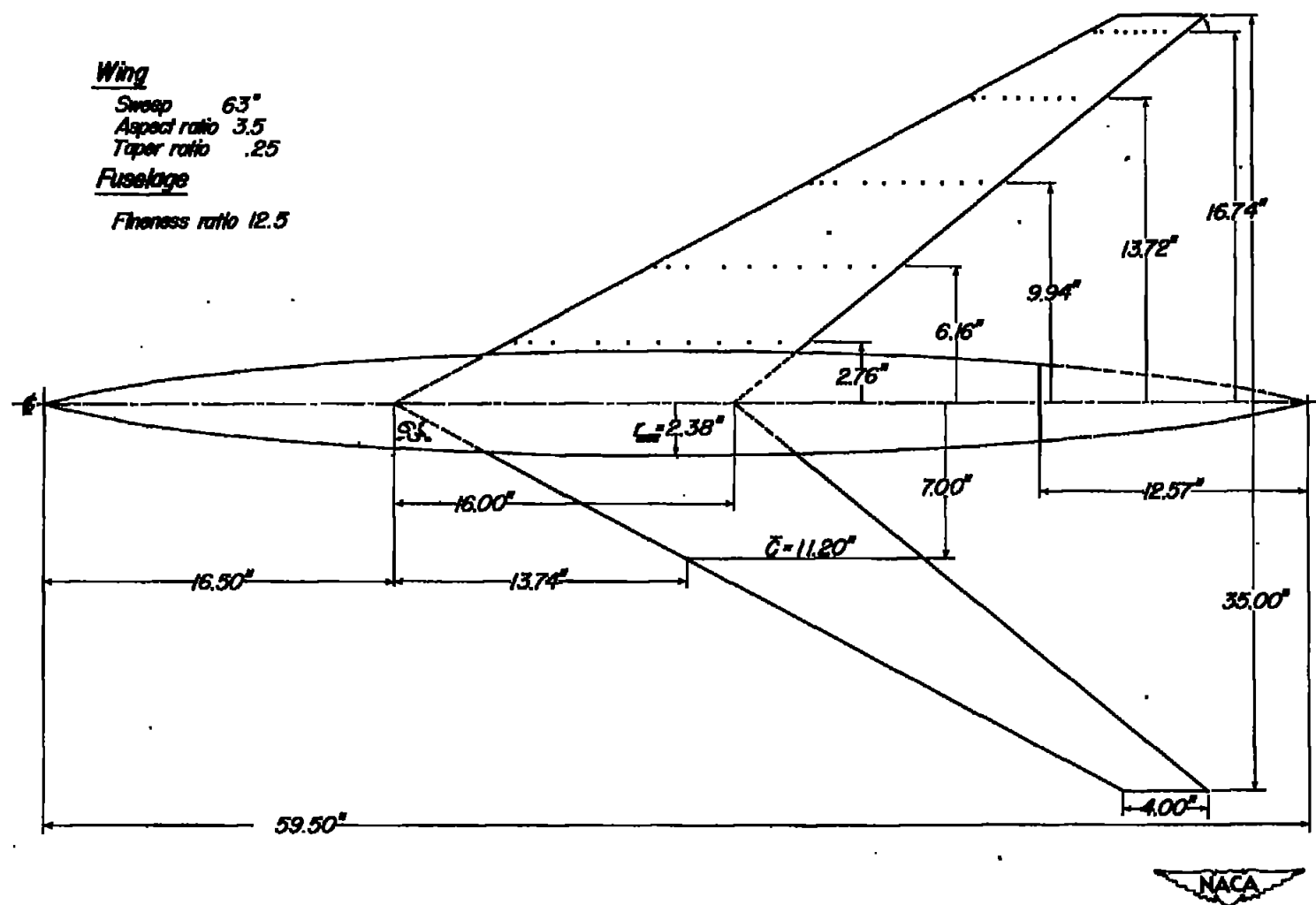


Figure 2.- General arrangement of model showing location of orifices.

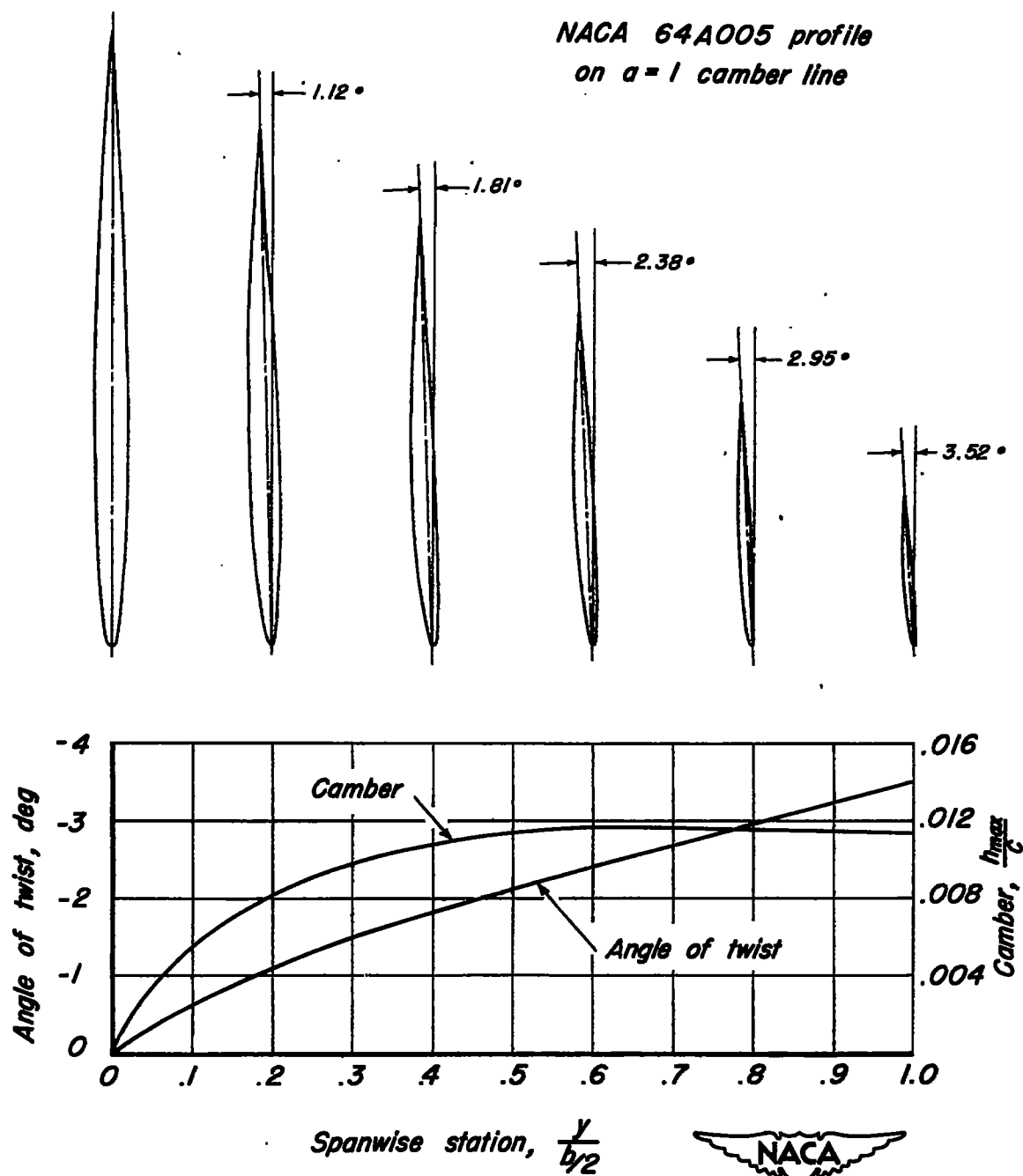


Figure 3.— Spanwise variation of wing twist and camber.

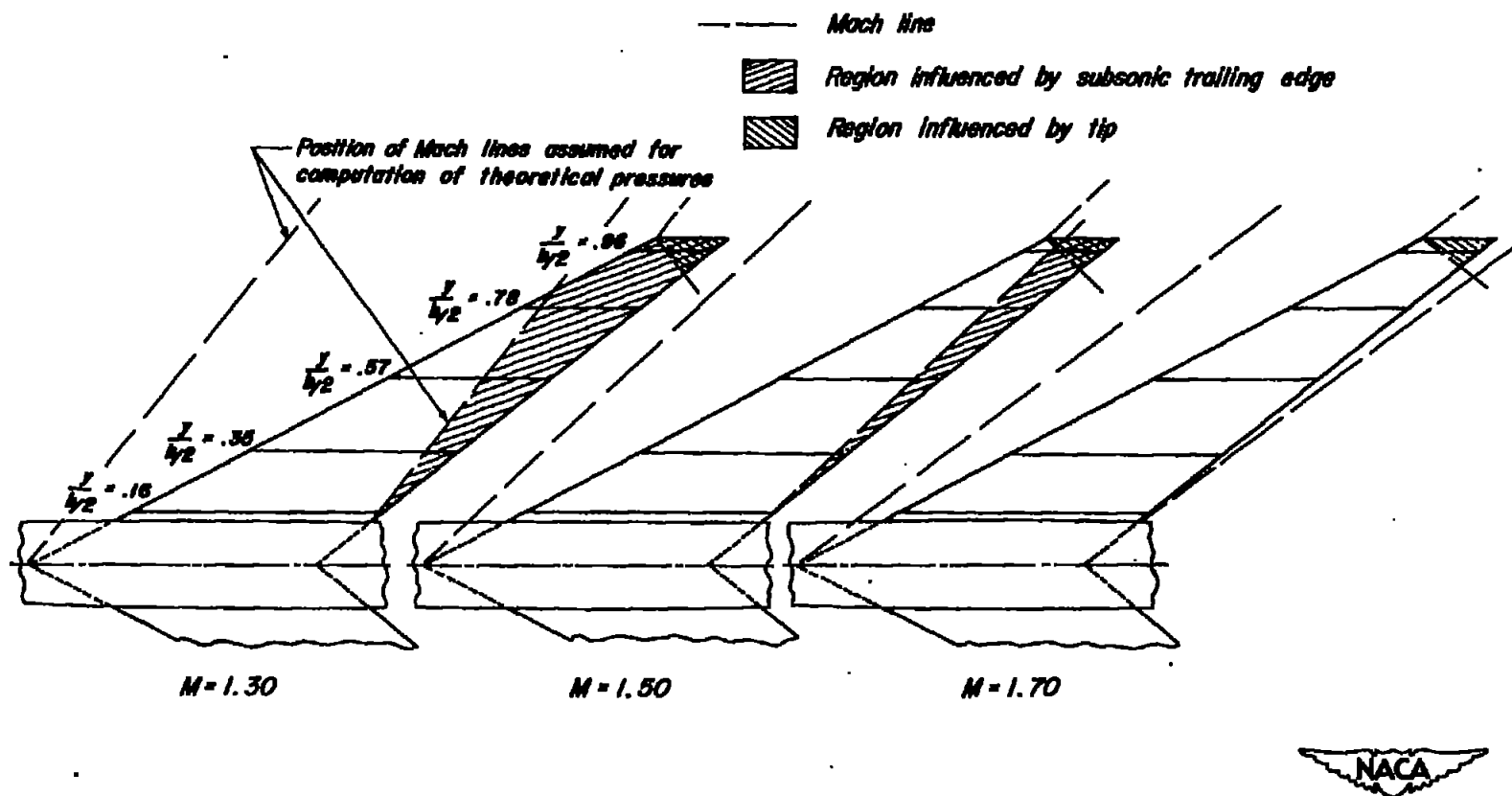


Figure 4.- Location of principal Mach lines relative to model for Mach numbers 1.30, 1.50, and 1.70.

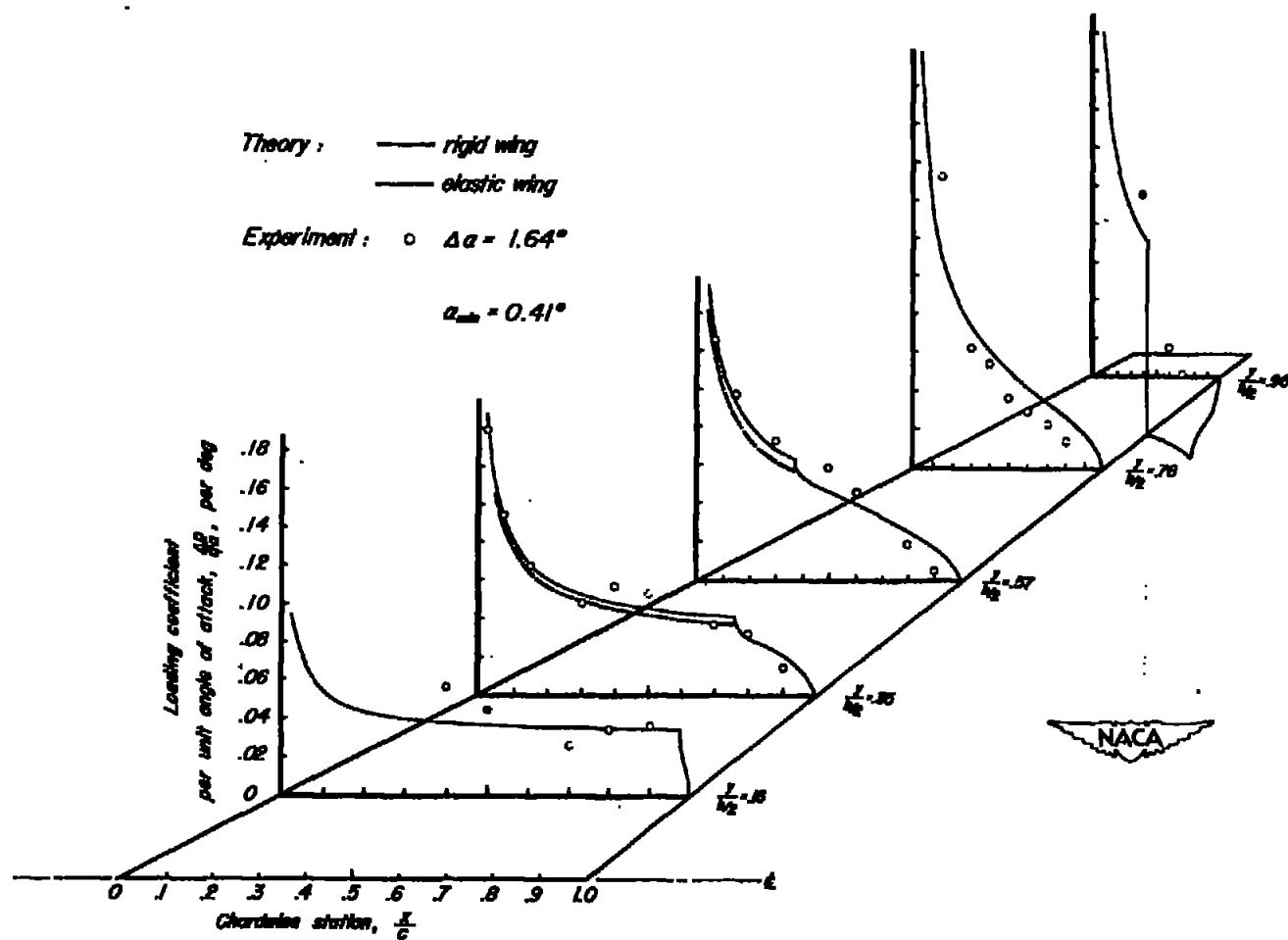


Figure 5.— Load distribution at Mach number 1.15.

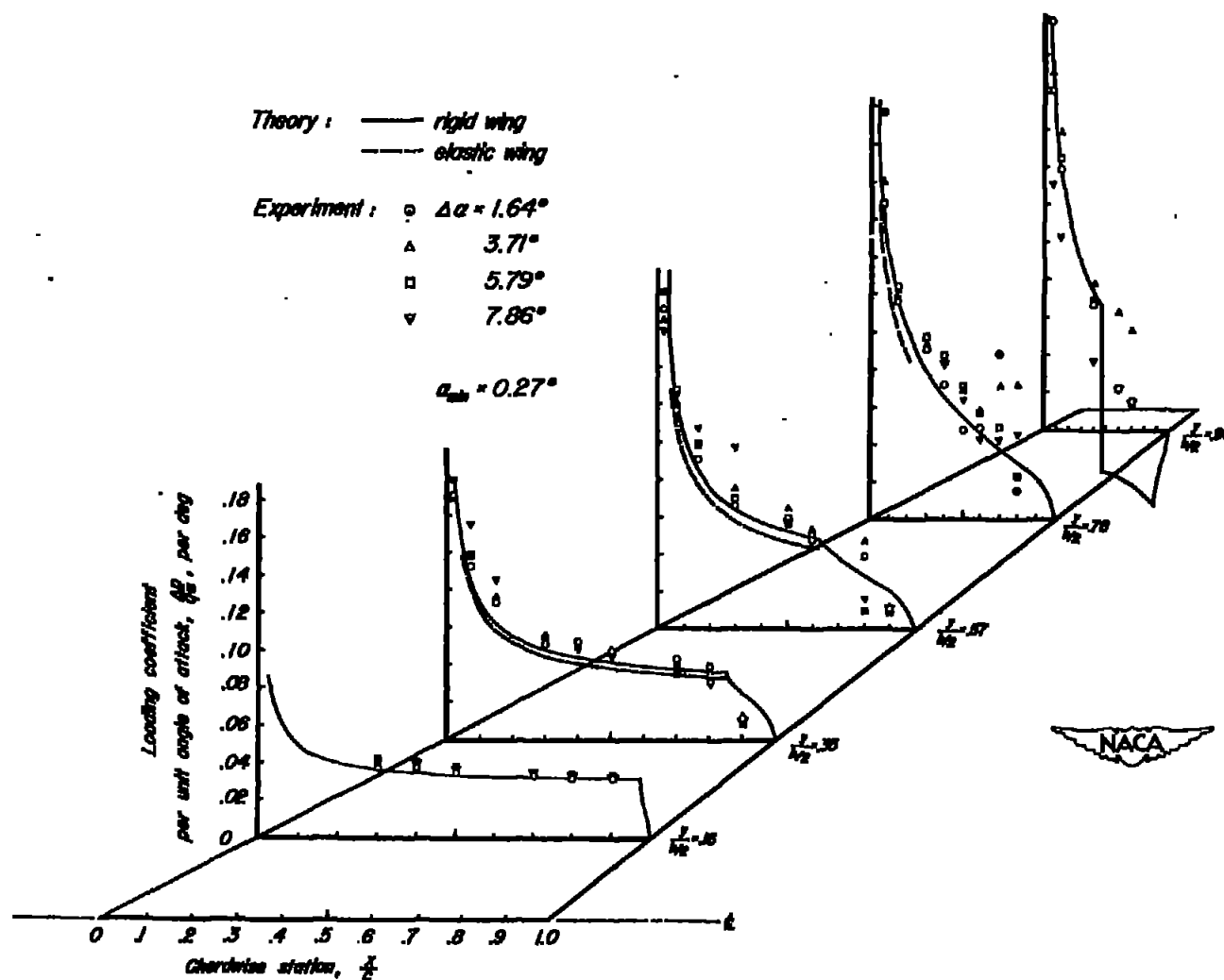


Figure 6.- Load distribution at Mach number 1.30.

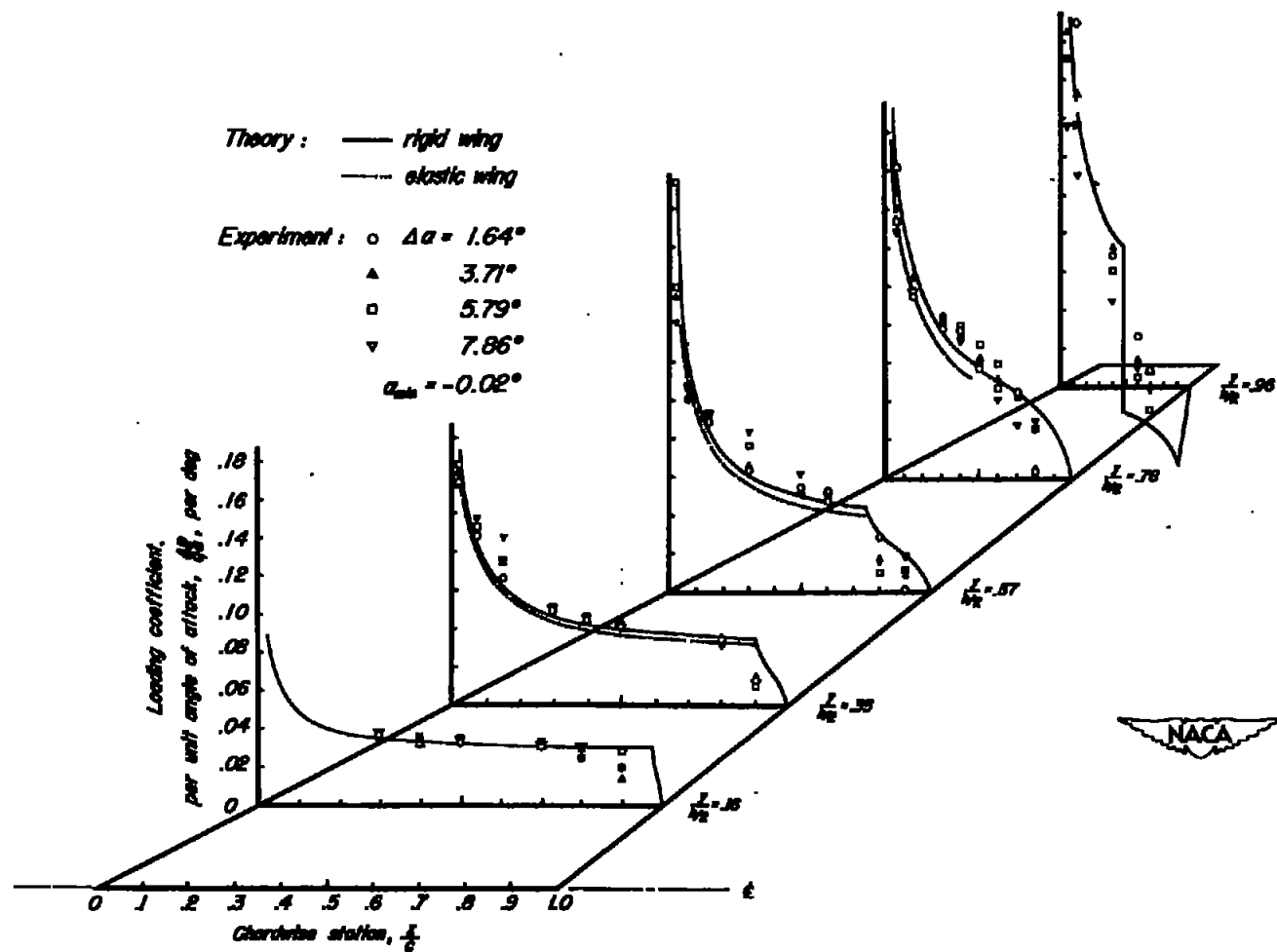


Figure 7.— Load distribution at Mach number 1.40.

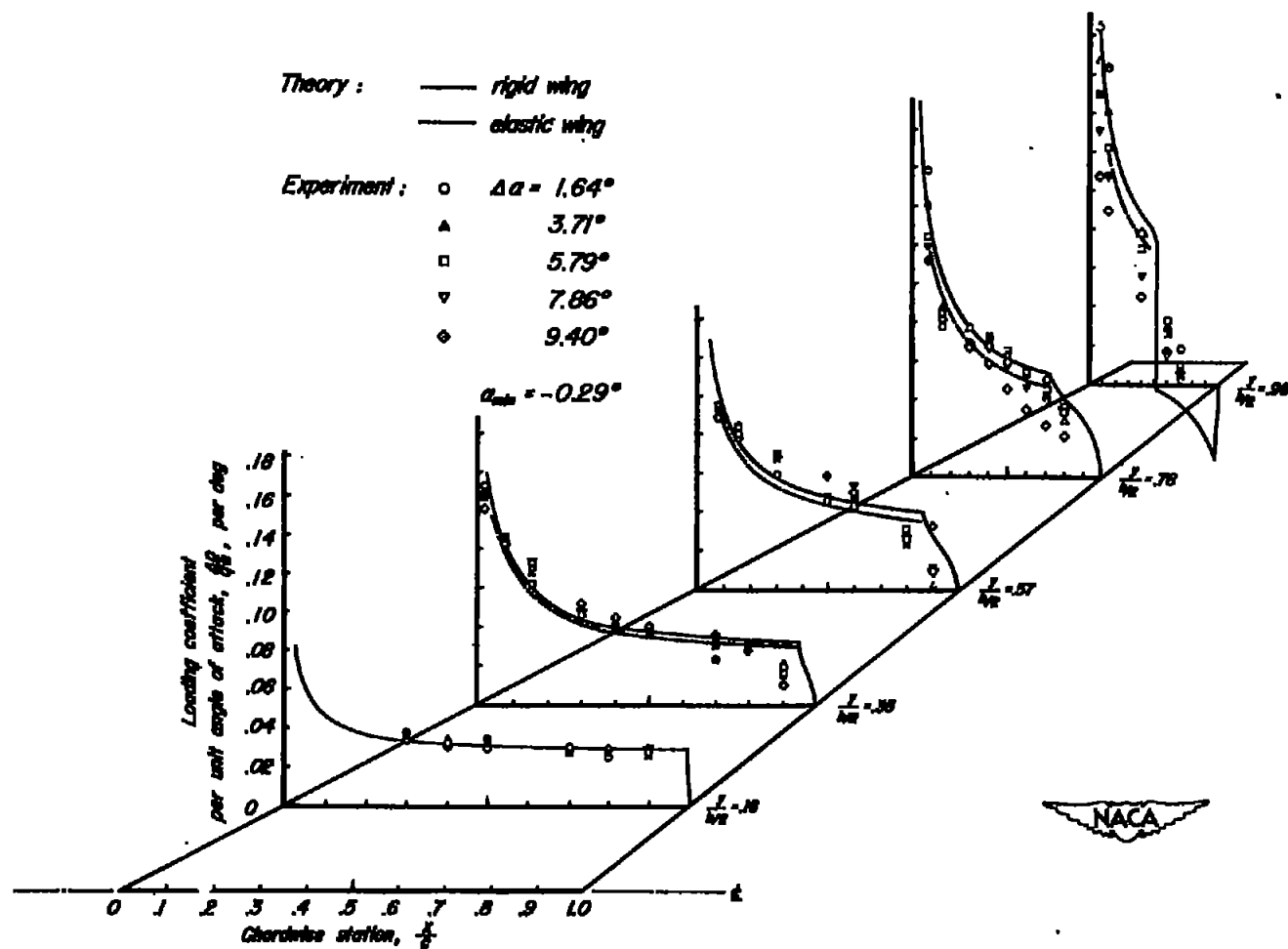


Figure 8.- Load distribution at Mach number 1.50.

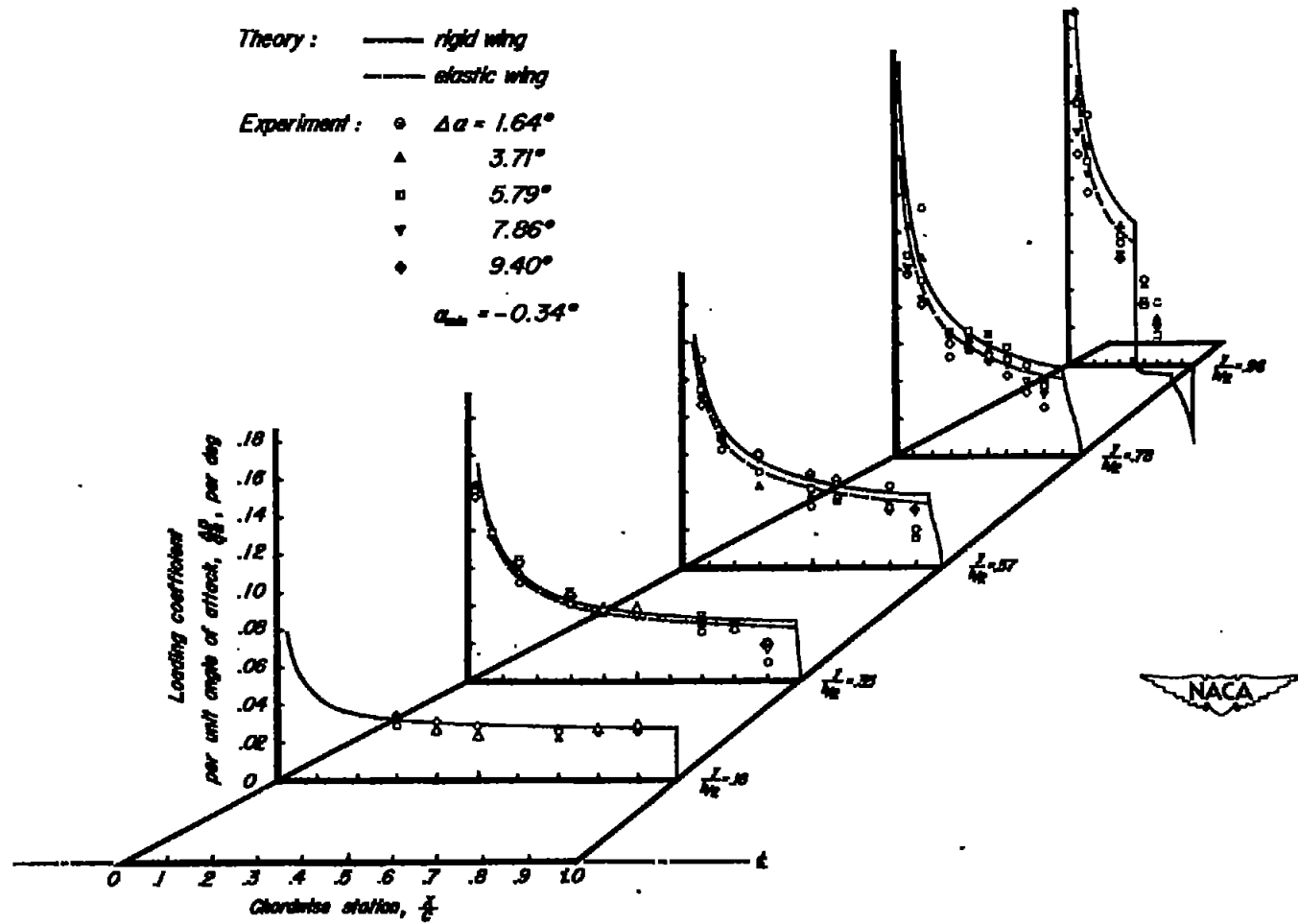


Figure 9.- Load distribution at Mach number 1.60.

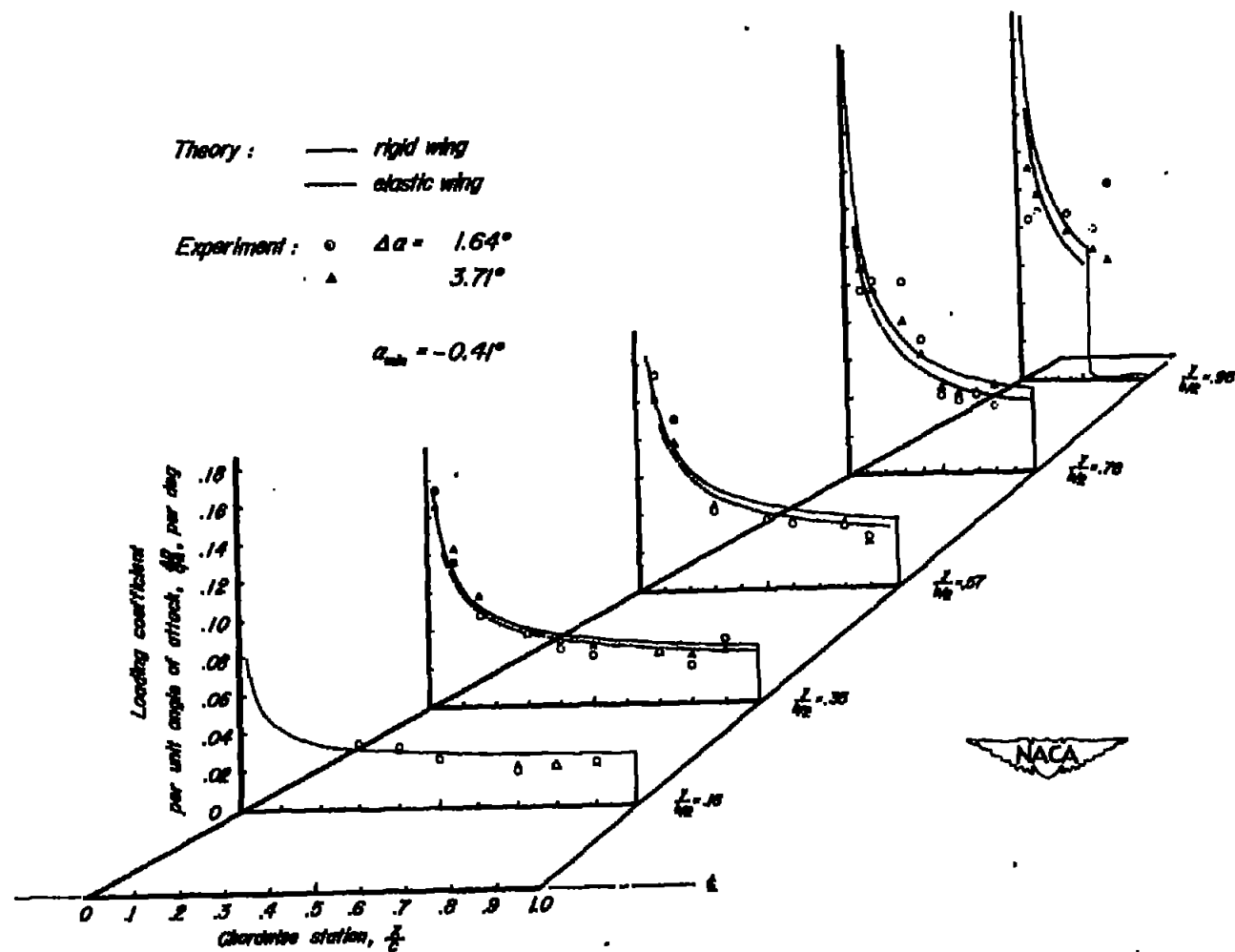


Figure 10.- Load distribution at Mach number 1.70.